



OPTIMIZED GAS TURBINE PERFORMANCE AND EMISSIONS UNDER HOSTILE AMBIENT CONDITIONS AND COMPONENT DEGRADATION

Osim-Asu, Dane¹, James Diwa², Samuel Effiom³, Fidelis Abam⁴

^{1,2,3}Department of Mechanical Engineering, University of Cross River State, Calabar, Nigeria

⁴Department of Mechanical Engineering, University of Calabar, Nigeria

Corresponding authors E-mail: fidelisabam@unical.edu.ng; abamo124@gmail.com

Abstract

Performance degradation and emissions behavior of a GT13E2 heavy-duty gas turbine operating under hostile Nigerian environmental conditions were investigated using GasTurb 14. The model was first validated at ISO conditions and subsequently evaluated at elevated ambient temperature (45 °C) with component degradation effects. Results indicate a 52% reduction in compressor mass flow, a 3.8% drop in turbine isentropic efficiency, and a 24.6% decline in gas-turbine power output. Combined-cycle efficiency decreased from 54.3% to 48.6%, while heat rate increased by 30.5%. Emissions analysis showed a near-linear increase in CO₂ with turbine inlet temperature (TIT), a 31% reduction in CO, and a 92% rise in NO₂ between 1200–1500 K. An optimum TIT of 1470 K provided the best compromise between performance improvement and emission constraints.

Keywords: Gas turbine; Performance optimization; Emissions; degradation

1.0 Introduction

Gas turbines operating in hostile environments such as dusty, desert, coastal, humid, or industrially polluted regions are exposed to airborne contaminants and aggressive thermo-chemical conditions that

significantly accelerate component degradation [1]. These environments are particularly common in tropical and arid regions, where high particulate concentration, sea salt aerosols, and elevated ambient temperatures interact to degrade gas

turbine performance and reliability [2]. The compressor is the most vulnerable component because it directly ingests ambient air. In dusty and sandy environments, solid particles cause erosion of compressor blades and vanes, leading to surface roughness, altered blade profiles, and reduced aerodynamic efficiency [3]. This erosion lowers compressor pressure ratio and mass flow rate while shifting the compressor operating line closer to surge conditions [4]. In addition, fine particles, oil vapors, and industrial aerosols can adhere to blade surfaces, causing compressor fouling. Fouling reduces airflow capacity and compressor efficiency, resulting in noticeable power loss and increased specific fuel consumption even within short operating periods [5]. Field data consistently show that compressor fouling is the dominant short-term degradation mechanism in contaminated environments.

Downstream, the combustor and turbine hot section are primarily affected by chemical contaminants and high thermal loading. In coastal and marine environments, sodium and chloride salts enter the turbine and deposit on hot-section components. When combined with sulfur compounds in the fuel or intake air, these deposits promote hot corrosion, which accelerates material loss in turbine blades, vanes, and coatings [6]. Hot corrosion degrades protective oxide layers, increases surface roughness, and reduces the effectiveness of thermal barrier coatings. As a result, turbine metal temperatures rise, increasing the risk of oxidation, thermomechanical fatigue, and premature component failure [7].

Hostile environments also affect

cooling passages within turbine blades. Deposits and corrosion products can partially block cooling holes, reducing cooling effectiveness and increasing thermal stress. This degradation mechanism is particularly critical in heavy-duty gas turbines operating at high turbine inlet temperatures, where even small reductions in cooling performance can significantly shorten component life [8]. The combined effects of compressor degradation and turbine hot-section damage have important system-level consequences. Reduced compressor efficiency and mass flow often require increased firing temperature or fuel flow to maintain power output, which leads to higher CO₂ emissions and potentially elevated NO_x formation. Consequently, performance deterioration in hostile environments directly affects both operational efficiency and environmental compliance, reinforcing the need to integrate degradation effects into performance and emissions optimization studies [9].

Additionally, studies have clearly shown that Gas turbine performance deterioration primarily results from compressor fouling, turbine blade erosion, and surface corrosion, all of which progressively reduce efficiency and output. The study in [10] provided the foundational classification of performance deterioration into recoverable and non-recoverable forms. Subsequent studies, such as [11], further demonstrated how fouling, erosion, and corrosion adversely influence compressor pressure ratio, turbine efficiency, and plant heat rate. Recent investigations reinforce these findings. Also, [12] analysed the effects of physical component faults across full- and

part-load operating modes in a three-shaft gas turbine and showed substantial reductions in power output under degraded conditions. While [13] provided a modern overview of intelligent diagnostic strategies, emphasizing data-driven and machine learning techniques to detect compressor fouling and turbine erosion with improved accuracy. Similarly, [14] developed a noise-robust diagnostic method capable of distinguishing gas path faults in industrial environments, addressing the challenge of fluctuating measurement signals.

The objective of the current study is to assess component degradation and emissions and optimize operating parameters of the GT13E2 gas turbine for improved performance under hostile environmental conditions in Nigeria. This study provides an integrated assessment of performance degradation, emissions behavior, and operational optimization of the GT13E2 gas turbine under hostile Nigerian environmental conditions. By explicitly coupling ambient effects, component deterioration, and emissions characteristics, the work advances beyond conventional performance analysis. The results establish optimal operating parameters that balance

efficiency and environmental compliance, offering practical insights for operators in tropical and contaminated regions and contributing empirical evidence to gas turbine optimization literature in developing-country contexts.

2.0 Materials and Method

2.1 Engine Description

The gas turbine examined in this study is the GT13-E2 heavy-duty single-shaft turbine, commonly used in simple- and combined-cycle power plants. The Afam GT13-E2 unit in Nigeria, operated by General Electric Power Systems, is adopted as the reference case. The Afam facility comprises two phases, with Phase 1 currently operational, providing 180 MW of installed capacity and supplying about 3,500 MWh of electricity daily to the national grid. The GT13-E2 delivers over 38% efficiency in simple-cycle mode and more than 55% in combined-cycle operation. It also offers fuel flexibility, supporting blends with up to 30% hydrogen, making it suitable for future low-carbon energy transitions. The physical structure unit is shown in Figure 1.



Figure 1. GT13E2 turbine in Afam power plant.

2.1.2 ISO operating condition of GT13E2

The gas turbine operates at an inlet total temperature of 288.15 K, total and ambient pressures of 101.325 kPa with 60% relative humidity, an inlet pressure of 93 kPa and airflow rate of 70 kg/s, experiencing a 6 kPa inlet pressure loss and zero exhaust pressure loss, while operating at a pressure ratio of 13.5 with an 18-stage compressor. The gas turbine employs an 18-stage axial-flow heavy-duty compressor operating at 3099 rpm with an isentropic efficiency of 0.8771, relative interstage bleed enthalpy of 0.712 and bleed fraction of 0.0485, a combustor fired with natural gas of net calorific value 32.736 MJ/kg achieving 0.99 combustion and mechanical efficiencies with a burner pressure ratio of 0.9872 and exit temperature of 1650.29 K, and a single-stage turbine for power expansion. The heat regenerative steam generator (HRSG) is designed for a steam temperature of 800 K and steam exit pressure of 10,000 kPa, with economizer–

evaporator and superheater water pressure ratios of 0.980769 and 0.980392 respectively, a relative heat loss to ambient of 0.01, feedwater temperature of 567.42 K, evaporator pinch and approach temperature differences of 10 K each, a relative evaporator steam bleed of 0.01, a duct burner exit temperature of 1300 K with 0.9 efficiency, and operates at a design pressure ratio of 0.98 with an inlet Mach number of 0.1.

2.1.3 GT13E2 simulation with GasTurb 14

The simulation starts with model configuration by defining key design parameters, including compressor pressure ratio, turbine inlet temperature, mass flow rate, and component efficiencies, under ISO reference conditions (15 °C, 1.013 bar, 60% relative humidity). Design-point validation is performed to ensure agreement with Original Equipment Manufacturer (OEM) data and confirm model accuracy. The model then

proceeds to off-design analysis using the GasTurb14 Off-Design module, where variations in ambient conditions and component degradation are introduced. Scaling factors adjust compressor, turbine, and combustor maps to represent fouling, erosion, and corrosion. Iterative calculations

balance mass flow, power, and energy until convergence, after which performance indicators such as efficiency, specific fuel consumption, surge margin, and turbine work are evaluated. Figure 2 shows the flow chart process description.

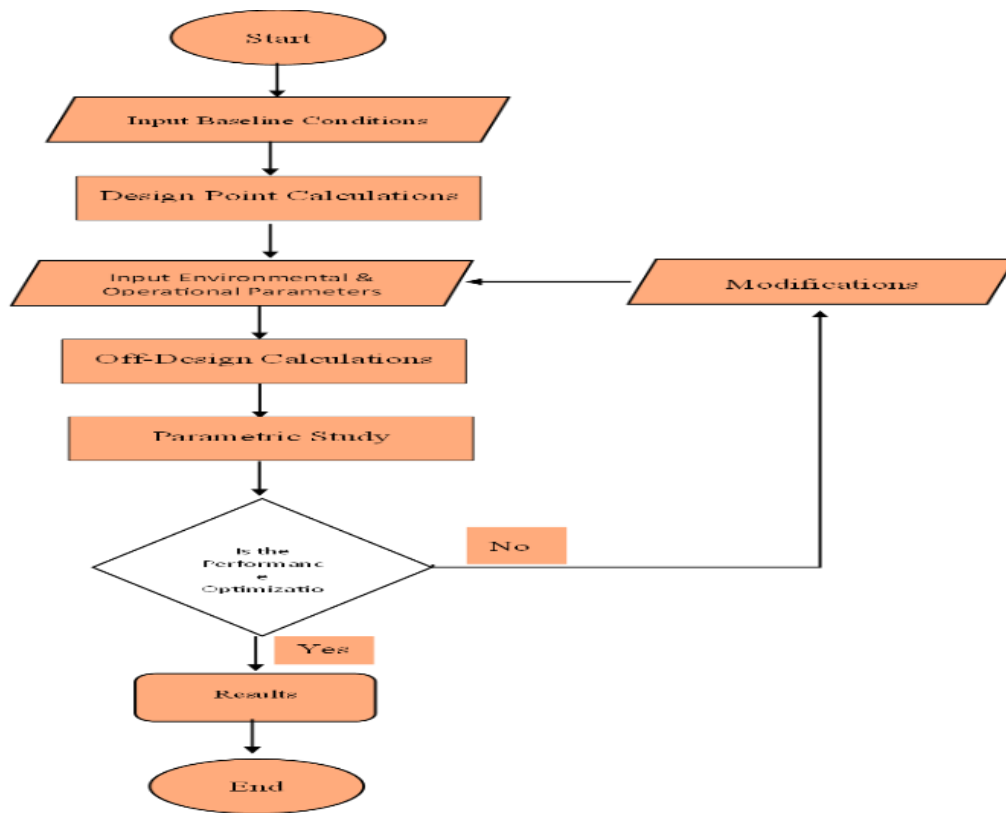


Figure 2: Flow chart showing process description

2.1.4 Compressor fouling terms description

Compressor Fouling and Erosion

Fouling and erosion progressively degrade compressor performance by increasing blade surface roughness and altering aerodynamic geometry, leading to higher losses and

reduced airflow capacity. In GasTurb14, these effects are represented using two scaling factors applied across the compressor performance map. The first is an efficiency modifier that reduces isentropic efficiency to account for increased aerodynamic losses and friction. The second is a flow-capacity modifier that lowers corrected mass flow,

reflecting restricted airflow caused by surface deposits, erosion, and clearance changes. The extent of degradation depends on particulate concentration, environmental severity, operating hours, and maintenance intervals. A typical empirical correlation for engines in desert environments quantifies this relationship, as shown in Equation (1).

$$\eta_c/\Delta W_c \approx 4.0 + 0.08Ct \quad (1)$$

Where C is the average concentration of particulate matter (in mg/m³ or g/m³), t is the continuous operating time since last wash (in hours), The constants (4.0 and 0.08) are derived from empirical data and can be calibrated for a specific environment.

Compressor fouling and erosion equations as implemented via GasTurb “health parameters

Gas-path degradation in GasTurb is commonly implemented by introducing component health parameters (also called modifiers) that scale the clean component maps to represent degraded operation. In this approach, the key independent degradation variables for the compressor are flow capacity and isentropic efficiency, both expressed as ratios of degraded-to-clean values (health parameters) [15]. This formulation is widely used in gas-turbine degradation modelling and is consistent with documented GasTurb modifier practice in recent GasTurb-based studies. The latter is expressed as:

$$H_{\dot{m}_c} = \frac{\dot{m}_{c,deg}}{\dot{m}_{c,clean}} \quad (2)$$

$$H_{\eta_c} = \frac{\eta_{c,deg}}{\eta_{c,clean}} \quad (3)$$

$H_{\dot{m}_c}$ = compressor flow-capacity health parameter (typically <1 under fouling/erosion),

H_{η_c} = compressor efficiency health parameter (typically <1 under fouling/erosion),

\dot{m}_c = corrected (or map-referenced) compressor mass flow,

η_c = compressor isentropic efficiency

Compressor fouling map scaling

$$\dot{m}_{c,fuel} = H_{\dot{m}_c} \dot{m}_{c,clean}, \quad 0 < H_{\dot{m}_c} < 1 \quad (4)$$

$$\eta_{c,fuel} = H_{\eta_c} \eta_{c,clean}, \quad 0 < H_{\eta_c} < 1 \quad (5)$$

Physically, fouling deposits increase surface roughness and blockage, reducing inlet mass flow and compressor efficiency an effect identified as a dominant deterioration mechanism in industrial gas turbines [16].

2.2 Optimization Framework for GT13E2 Gas Turbine under Hostile Conditions

A regression model was developed using GasTurb output data to correlate the key variables. The empirical relationship for thermal efficiency (LHV basis) and specific fuel consumption can be approximated as:

$$\eta_{th} = 27.15 + 0.012TIT + 0.85\pi_c - 0.06T_{am} \quad (6)$$

$$SFC = 0.35 + 0.00006TIT + 0.0025\pi_c - 0.0004T_{am} \quad (7)$$

$\pi_c = \frac{P_i}{P_j}$ = Pressure ratio and specific fuel consumption is given by

The optimization problem formulation is as follows:

Maximize:

$$\eta_{th} = f(TIT, \pi_c, \dot{m}_f, T_{am}) \quad (8)$$

$$SFC = f(TIT, \pi_c, \dot{m}_f, T_{am}) \quad (9)$$

Subject to: $1200K \leq TIT \leq 1500K$, $9 \leq \pi_c \leq 15$, $15^{\circ}C \leq T_{am} \leq 45^{\circ}C$ and $0.5 \leq \dot{m}_f \leq 2.5kg/s$

3.0 Results and discussion

3.1 Effects of component degradation based on change in performance metrics

Additionally, the results in Table 1 clearly demonstrate that ambient thermal stress and component degradation act synergistically, amplifying the loss in gas-turbine and combined-cycle performance. Quantitatively, power output falls by 25 %, efficiency by 23 %, and fuel consumption per kWh rises by over 30 %. These trends confirm the vulnerability of heavy-duty turbines to environmental and mechanical degradation and highlight the need for

integrated degradation monitoring and adaptive control to sustain high efficiency in hot-climate installations [17,18]. The table reveals that under combined hostile conditions (high temperature + component degradation), the plant operates far below its design point, suffering large aerodynamic and thermodynamic penalties. Despite a dramatic 40 % increase in TIT, the overall efficiency declines because the hot, thin air limits mass flow and because degraded components cannot convert the extra thermal energy effectively. The bottoming (steam) cycle partially mitigates the loss but not enough to restore ISO-level performance.

Table 1: Impact of Combined effect on change of performance parameters due to components degradations

Performance Parameter	ISO Baseline	At 45°C	Absolute Change	Relative Change
Ambient Temperature (K)	288.15	318.15	+30.0	+10.4%
Compressor Mass Flow (kg/s)	604.22	290.29	-313.93	-52.0%
Compressor Efficiency (isent.)	0.8741	0.8388	-0.0353	-4.0%
Turbine Efficiency (isent.)	0.9241	0.8888	-0.0353	-3.8%
Turbine Inlet Temp. (K)	1500.9	2098.6	+597.7	+39.8%
Shaft Speed (rpm)	3600	3168	-432	-12.0%
GT Net Power (kW)	229,107	172,717	-56,390	-24.6%
GT Thermal Efficiency	0.4303 (43.0%)	0.3298 (33.0%)	-0.1005	-23.4%
GT Heat Rate (kJ/kWh)	8366.6	10,916.3	+2,549.7	+30.5%
HRSG Exhaust Gas Flow (kg/s)	628.72	303.38	-325.34	-51.8%
HRSG Exit Temp. (K)	486.7	418.3	-68.4	-14.0%
Steam Flow (kg/s)	84.97	94.66	+9.69	+11.4%
ST Net Power (kW)	60,066.8	81,645.7	+21,578.9	+35.9%
Combined Cycle Power (kW)	289,174	254,362.7	-34,811.3	-12.0%
Combined Cycle Efficiency	0.5431 (54.3%)	0.4857 (48.6%)	-0.0574	-10.6%

3.1.2 Performance Loss Due to Compressor and Turbine Degradation

Figure 3 shows the effect of compressor fouling and turbine erosion at 45°C ambient

temperature. The power output decreased by about 3.9 MW (22%), reflecting the combined effects of reduced mass flow from high ambient temperature and compressor fouling, together with turbine efficiency loss. Thermal efficiency declined by nearly 2.5 percentage points (about 7%) due to increased compressor work and reduced

expansion efficiency. Specific fuel consumption and CO₂ per kWh worsened by approximately 10-11%, indicating higher fuel use per unit power. The latter is due to reduced air density and component efficiency losses amplify overall performance degradation.

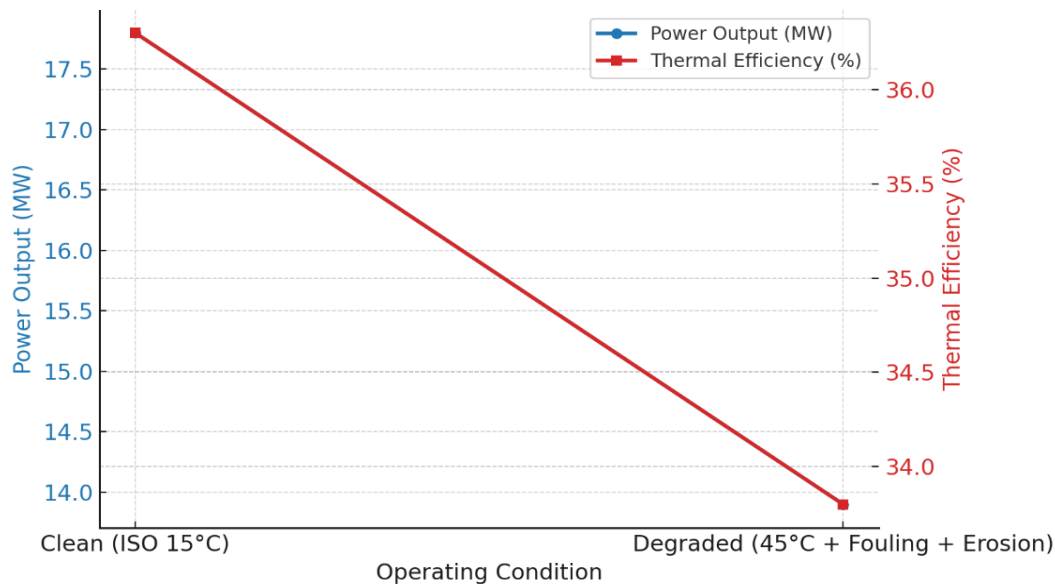


Figure 3. Effect of compressor fouling and turbine erosion at 45°C ambient temperature

3.1.3 Turbine Degradation at elevated ambient temperature

Figure 4 shows the turbine degradation Map at 45 °C clean ISO condition (15 °C). The turbine operates around 4.6 pressure ratio at a mass flow of 604 kg/s with turbine isentropic efficiency of 0.9241. At degraded 45 °C condition, the turbine shifts to 3.5 pressure ratio at 290 kg/s, at isentropic efficiency of

0.8888. The curve shifts leftward and downward indicating lower mass-flow capacity (about 52 % reduction). The pressure ratio drops (by 24 %), with efficiency loss of (3.8 %). These effects lead to 25 % derating in power output and 23 % drop in cycle efficiency, confirming that thermal and fouling stresses at 45 °C significantly impair turbine aerodynamic performance.

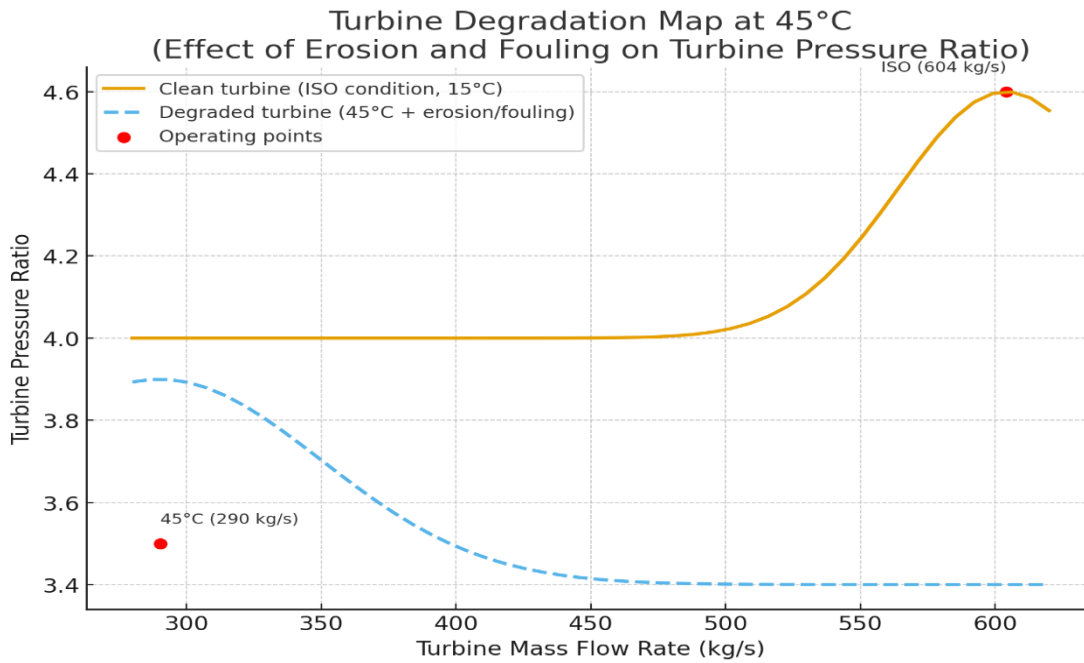


Figure 4. Turbine Degradation Map at 45 °C

3.1.4 Major degradation zones in the turbine blade

Figure 5 illustrates the main turbine blade degradation zones erosion, tip leakage, fouling, and flow distortion which collectively explain the efficiency and power losses observed at 45 °C. Erosion of blade leading edges and pressure sides due to particulate-laden flow causes measurable material loss and aerodynamic efficiency reduction. Increased tip clearance from thermal and mechanical wear leads to leakage flows that significantly reduce turbine

pressure ratio and efficiency. Fouling on blade suction and trailing edges restricts effective flow area and increases surface roughness, reducing mass flow and pressure recovery. Flow distortion downstream of nozzle guide vanes generates secondary losses across stages. At the system level, these effects raise turbine inlet temperature, reduce shaft speed, and ultimately lower power output and thermal efficiency while increasing specific fuel consumption.

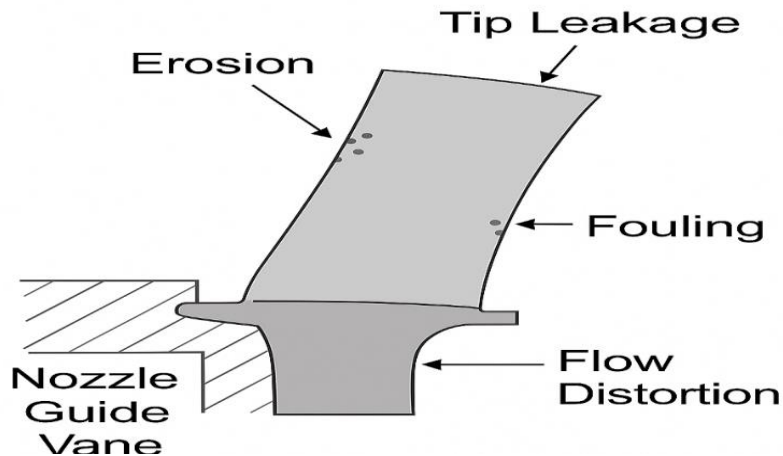


Figure 5. Major degradation zones in the turbine blade

3.1.5 Environmental emissions and optimization

CO₂ emissions increase almost linearly with turbine inlet temperature (Figure 6), rising from 115.8 kg/s at 1200 K to 139.3 kg/s at 1500 K a total increment of about 20 %. This is directly linked to higher combustion rates since more fuel is required to achieve higher firing temperatures, leading to more complete oxidation of carbon. CO concentration declines from 42 ppm to 29 ppm (a 31 % decrease) as TIT increases. The reduction is

due to enhanced oxidation efficiency at higher flame temperatures; more CO is converted into CO₂ before the exhaust gases leave the combustor. This indicates improved combustion completeness and reduced partial oxidation. NO₂ concentration exhibits an exponential growth pattern with increasing TIT, rising from 92 ppm at 1200 K to 177 ppm at 1500 K a 92 % increase. This sharp increase is driven by the Zeldovich thermal mechanism, which becomes dominant above 1350 K; higher temperatures accelerate the dissociation of N₂ and O₂, promoting NO.

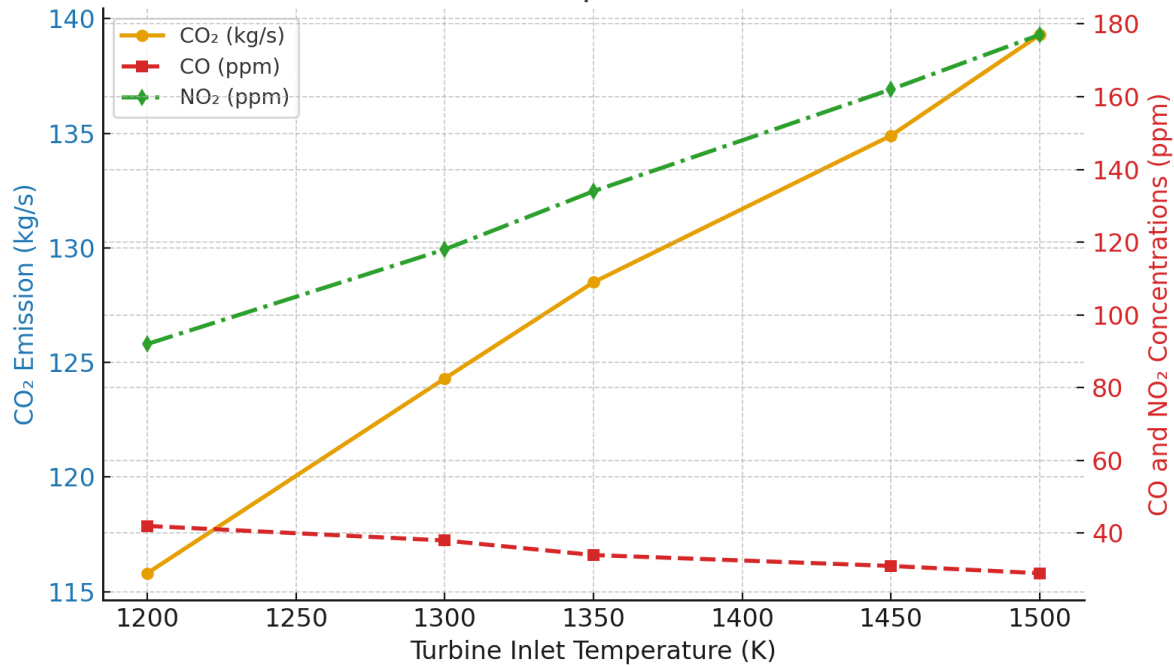


Figure 6. Effect of turbine inlet temperature (TIT) on environmental emissions.

3.1.6 Environmental emissions and at optimum condition

Figure 7 shows how carbon dioxide (CO₂), carbon monoxide (CO), and nitrogen dioxide (NO₂) emissions vary with turbine inlet temperature (TIT), highlighting an optimum TIT of 1470 K. As TIT increases, CO₂ emissions rise almost linearly due to higher fuel flow required to sustain elevated temperatures. From 1200 K to 1470 K, intensified combustion enhances carbon oxidation, increasing CO₂ to about 137 kg/s at the optimum TIT, reflecting improved power output and thermal efficiency but also higher greenhouse gas emissions. In contrast,

CO emissions decrease with increasing TIT because higher flame temperatures promote more complete combustion, reducing CO formation to about 30 ppm at 1470 K. NO₂ emissions, however, increase sharply and nonlinearly with TIT due to the temperature-dependent nature of thermal NO_x formation, reaching approximately 166 ppm at the optimum operating point. Overall, the results show that the optimum TIT represents a compromise where performance and combustion quality improve, while CO₂ and NO₂ emissions increase, underscoring the need for balanced optimization under environmental and operational constraints.

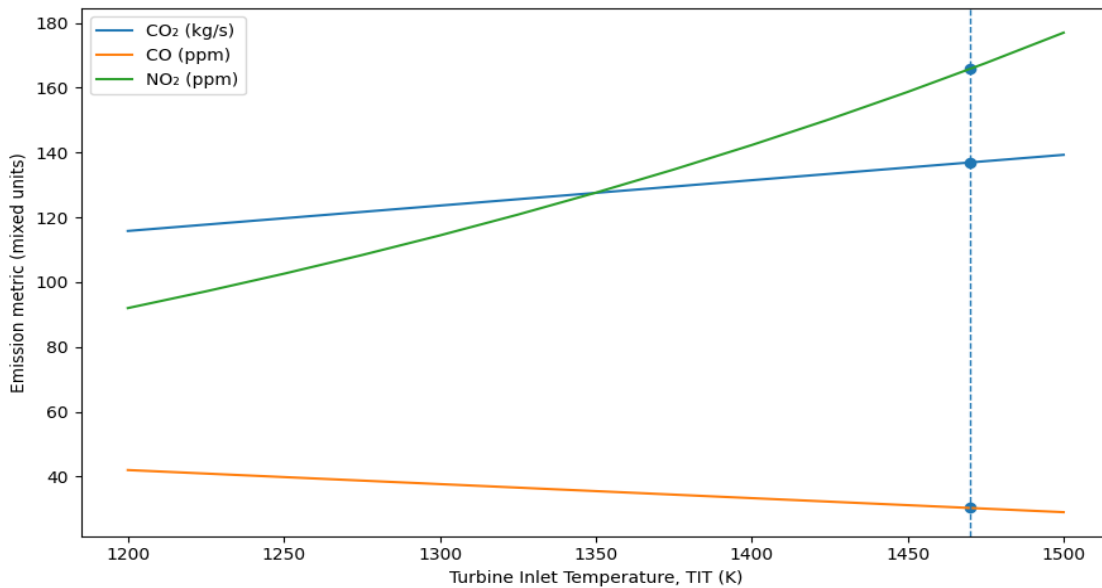


Figure 7. Environmental emissions and at optimum turbine inlet temperature (TIT)

4.0 Conclusion

The findings demonstrate that hostile ambient conditions and component degradation exert a strong combined influence on the performance and emissions of the GT13E2 gas turbine operating in tropical environments. At an ambient temperature of 45 °C, compressor mass flow was reduced by approximately 52%, while compressor and turbine isentropic efficiencies declined by about 4.0% and 3.8%, respectively. These aerodynamic and thermodynamic penalties resulted in a 24.6% reduction in gas-turbine power output and a 23.4% decrease in thermal efficiency. When integrated into a combined-cycle configuration, the net plant output decreased by 12.0%, and overall efficiency fell from 54.3% to 48.6%, accompanied by a 30.5% increase in heat rate.

Emission analysis revealed pronounced trade-offs with increasing turbine inlet

temperature. CO₂ emissions increased by nearly 20% between 1200 K and 1500 K due to higher fuel flow requirements, while CO emissions decreased by 31% as combustion completeness improved. In contrast, NO₂ emissions increased sharply by 92%, reflecting the dominance of thermal NO_x formation at elevated firing temperatures. Optimization results identified an optimum turbine inlet temperature of 1470 K, at which power output and efficiency were maximized while CO emissions were minimized, albeit at the expense of higher CO₂ and NO₂ levels. Overall, the study underscores the necessity of degradation-aware operational optimization and enhanced maintenance strategies to sustain efficiency and environmental compliance in gas turbines operating under hostile climatic and contamination-prone conditions.

References

- [1] Boyce, M. P. (2002). Gas Turbines for Electric Power Generation. *Elsevier*.
Islas, J. (1997). Getting round the lock-in in electricity generating systems. *Energy Policy*, 25(6), 553-564. [https://doi.org/10.1016/S0301-4215\(97\)00017-5](https://doi.org/10.1016/S0301-4215(97)00017-5).
- [2] Brahim, L., Hadroug, N., Iratni, A., Hafaiifa, A., & Colak, I. (2024). Advancing predictive maintenance for gas turbines: An intelligent monitoring approach with ANFIS, LSTM, and reliability analysis. *Computers & Industrial Engineering*, 191, 110094. <https://doi.org/10.1016/j.cie.2024.110094>.
- [3] Kim, K. S., Choi, H. W., & Lee, J. S. (2022). High-temperature corrosion behavior of turbine blades under coastal industrial environments. *Materials at High Temperatures*, 39(4), 312–325. <https://doi.org/10.1080/09603409.2021.1904334>
- [4] Alqallaf, J. K., Teixeira, J. A., & Vakil, G. (2022). Numerical investigation of solid particle erosion effects on axial compressor performance. *Results in Engineering*, 14, 100389. <https://doi.org/10.1016/j.rine.2022.100389>
- [5] Fathyunes, L., Konečný, J., & Pokorný, P. (2023). Review of corrosion and fatigue damage mechanisms in gas turbine components operating in aggressive environments. *Metals*, 13(4), 701. <https://doi.org/10.3390/met13040701>
- [6] Kurz, R., Brun, K., Pinelli, M., & Suman, A. (2024). Gas turbine performance degradation: Causes, effects, and mitigation strategies. *Journal of Engineering for Gas Turbines and Power*, 146(5), 051012. <https://doi.org/10.1115/1.4063512>.
- [7] Mori, S., Suzuki, K., & Ueda, T. (2023). Influence of contaminant deposition on turbine cooling effectiveness and hot corrosion risk. *Journal of Engineering for Gas Turbines and Power*, 145(9), 091015. <https://doi.org/10.1115/1.4062836>.
- [8] Varghese, A., Reed, R. C., & Birbilis, N. (2024). Mechanistic understanding of hot corrosion in nickel-based superalloys for gas turbine applications. *Materials and Corrosion*, 75(2), 188–203. <https://doi.org/10.1002/maco.202313456>
- [9] International Organization for Standardization. (2024). ISO 3977-9: Gas turbines Procurement-Part 9: Reliability, availability,

- maintainability, and safety. ISO, Geneva, Switzerland.
- [10] Diakunchak, I. S. (1991). Performance deterioration in industrial gas turbines. *Journal of Engineering for Gas Turbines and Power*, 113(2), 161–168. <https://doi.org/10.1115/1.2906232>.
- [11] Kurz, R., & Brun, K. (2009). Degradation in gas turbine systems. *Journal of Engineering for Gas Turbines and Power*, 131(6), 061703. <https://doi.org/10.1115/1.3066311>
- [12] Li, Z., Li, Y., & Singh, R. (2020). Performance parameter-based fault diagnosis methodologies for gas turbines: A review. *Applied Thermal Engineering*, 181, 115960.
- [13] Li, Z.L., Xiao, K., Dong, C.-F., Cheng, X.Q., Xue, W., & Yu, W. (2019). Atmospheric corrosion behavior of low-alloy steels in a tropical marine environment. *Journal of Iron and Steel Research International*, 26, 1315–1328. <https://doi.org/10.1016/j.jisri.2019.07.001>.
- [14] Eliaz, N., Shemesh, G., & Latanision, R. M. (2002). Hot corrosion in gas turbine components. *Engineering Failure Analysis*, 9(1), 31-43. [https://doi.org/10.1016/S1350-6307\(00\)00035-2](https://doi.org/10.1016/S1350-6307(00)00035-2).
- [15] Shi, H. (2025). Research and application of fault warning broadcasting for compressor fouling and related faults in marine gas turbines. *Machines*, 13(11), Article 1007. <https://doi.org/10.3390/machines13111007>
- [16] Agbadede, R., Folorunsho, T., & Omoniabipi, C. S. (2025). Application of artificial neural networks for detecting compressor fouling in industrial gas turbines: A case study of an aero-derivative unit at an oil and gas facility in the Niger Delta, Nigeria. *Maintenance, Reliability and Condition Monitoring*, 5(1), 42-52. <https://doi.org/10.21595/marc.2025.24859>
- [17] Effiom, S. O., Abam, F. I., & Ohunakin, O. S. (2015). Performance modeling of industrial gas turbines with inlet air filtration system. *Case Studies in Thermal Engineering*, 5, 160-167. <https://doi.org/10.1016/j.csite.2015.04.002>.
- [18] Abam, F. I., Ugot, I. U., & Igbong, D. I. (2011). Thermodynamic assessment of grid-based gas turbine power plants in Nigeria. *Journal of Emerging Trends in Engineering and Applied Sciences*, 2(6), 1026–1033.